Reconstruction Control of Magnetic Properties during Epitaxial Growth of Ferromagnetic $Mn_{3-\delta}Ga$ on Wurtzite GaN(0001)

Erdong Lu, David C. Ingram, and Arthur R. Smith

Nanoscale and Quantum Phenomena Institute, Department of Physics and Astronomy, Ohio University, Athens, Ohio 45701, USA

J. W. Knepper and F. Y. Yang

Department of Physics, The Ohio State University, 191 Woodruff Avenue, Columbus, Ohio 43210, USA

(Received 16 July 2006; published 2 October 2006)

Binary ferromagnetic $Mn_{3-\delta}Ga$ ($1.2 < 3 - \delta \leq 1.5$) crystalline thin films have been epitaxially grown on wurtzite GaN(0001) surfaces using rf *N*-plasma molecular beam epitaxy. The film structure is face-centered tetragonal with CuAu type-I ($L1_0$) ordering with (111) orientation. The in-plane epitaxial relationship to GaN is nearly ideal with $[1\bar{1}0]_{MnGa} \parallel [1\bar{1}00]_{GaN}$ and $[11\bar{2}]_{MnGa} \parallel [11\bar{2}0]_{GaN}$. We observe magnetic anisotropy along both the in-plane and out-of-plane directions. The magnetic moments are found to depend on the Mn/(Mn + Ga) flux ratio and can be controlled by observation of the surface reconstruction during growth, which varies from 1×1 to 2×2 with increasing Mn stoichiometry.

DOI: 10.1103/PhysRevLett.97.146101 PACS numbers: 68.55.Jk, 68.37.Ef, 75.70.−i, 81.15.Hi

In the past two decades, there have been many attempts to grow crystalline, tetragonal ferromagnetic (FM) Mn_xGa_{1-x} thin films on a GaAs(100) semiconductor (SC) by molecular beam epitaxy (MBE) [1–6] and, mostly in recent years, to try different ways to fabricate new materials such as Mn-doped GaAs and GaN as dilute FM semiconductors with a potential use in spintronics [7–11]. By comparison, there have been very few attempts to grow epitaxial FM layers on wide band-gap semiconductors such as GaN, although such FM/SC structures have great potential for novel applications, such as for spin light-emitting diodes operating in the blue and ultraviolet (UV) spectral ranges [11,12].

Mn and Ga are known to form different bulk alloy phases, even a quasicrystalline phase, depending on the ratio of Mn to Ga and the temperature during crystal growth and preparation [13–18]. Many phases with Mn greater than or equal to Ga are FM with a high Curie temperature (T_C) above room temperature, for example, Mn_3Ga with $T_C = 470\,^\circ$C, Mn_2Ga with $T_C = 417\,^\circ$C, and MnGa with $T_C > 27\,^\circ$C [8,19]. The "δ phase" $Mn_{3-\delta}Ga$, with δ in the range 1.5–1.8, is very promising for spintronic applications due to the high magnetic moment; theoretically, it can be as high as $2.5\mu_B$. However, to realize the potential of δ-MnGa for blue and UV spintronic devices, it is essential to explore the magnetic and structural properties and their epitaxial growth dependence for thin $Mn_{3-\delta}Ga$ layers on wide band-gap semiconductor (i.e., GaN) and insulating (i.e., MgO or Al_2O_3) surfaces.

In this Letter, we present new results for $Mn_{3-\delta}Ga$ thin layers grown smoothly on *w*-GaN, both nitrogen-polar $(000\bar{1})$ and gallium-polar (0001) substrates. We identify a growth regime which results in near-perfect heteroepitaxy with a well-defined epitaxial film-substrate relationship, a high quality film-substrate interface, and excellent magnetic properties. We show that the film structure can be understood in terms of the (111) face of the well-known face-centered tetragonal (fct) CuAu type-I ($L1_0$) model for δ-MnGa [13]. While we report magnetic properties of these layers as high as any previously reported values for $Mn_{3-\delta}Ga$, we furthermore show that the magnetic properties can be tuned during MBE growth by monitoring the surface structure and adjusting the flux ratio.

The experiments are performed in a custom-designed, ultrahigh vacuum (UHV) scanning tunneling microscope (STM)/MBE system having Mn and Ga effusion cells and a radio-frequency (rf) nitrogen (N_2) plasma source. Mn and Ga fluxes are measured using a quartz crystal thickness monitor. Reflection high energy electron diffraction (RHEED) is used to monitor the growth surface.

Ga-polar substrates used were *w*-GaN grown on sapphire [Al_2O_3(0001)] using metal-organic chemical vapor deposition by a commercial vendor, whereas the *N*-polar substrates were grown on Al_2O_3(0001) in the lab using rf *N*-plasma MBE. The Ga-polar substrates were treated (keeping the same polarity) in vacuum by either heating to 650 °C or by growing a fresh 50-nm layer of GaN. *N*-plasma GaN growth conditions were $T_{sub} = 650\,^\circ$C, $P_{N_2} = 9.1 \times 10^{-6}$ Torr, and Ga flux $J_{Ga} = 3.87 \times 10^{14}/\text{cm}^2$ sec. Following substrate preparation, the substrate temperature was set to $T_{sub} = 250\,^\circ$C for the $Mn_{3-\delta}Ga$ growth. The flux ratio $R_F = J_{Mn}/(J_{Mn} + J_{Ga})$ was set to achieve a particular stoichiometry within the range of 0.5–0.6, corresponding to a Mn:Ga ratio in the range 2:2–3:2.

Here we focus on two cases, one with $R_F = 0.5$ for Mn:Ga = 1:1($\delta = 2$) and one with $R_F = 0.55$ for Mn:Ga = 1.22:1($\delta = 1.78$). Other samples were grown with $R_F = 0.60$, finding similar results as for 0.55. For $R_F = 0.5$, the fluxes of Mn and Ga—J_{Mn} and J_{Ga}—are both set at $2.87 \times 10^{14}/\text{cm}^2$ sec. For $R_F = 0.55$, the fluxes are set at $J_{Mn} = 2.87 \times 10^{14}/\text{cm}^2$ sec and $J_{Ga} = 2.35 \times 10^{14}/\text{cm}^2$ sec. Following $Mn_{3-\delta}Ga$ growth, the samples are transferred under UHV to the *in situ* STM. Samples are

analyzed *ex situ* using x-ray diffraction (XRD), Rutherford backscattering spectroscopy (RBS), and vibrating sample magnetometry (VSM).

Figures 1(a) and 1(b) show typical RHEED patterns for a *w*-GaN(0001) surface just after growth of a fresh 50 nm GaN layer followed by cooling down to the $Mn_{3-\delta}Ga$ growth temperature $T_{S,MnGa} = 250\,^{\circ}C$. The apparent Ga-polar, pseudo-1×1 reconstruction suggests a smooth GaN(0001) surface [20].

RHEED patterns of the subsequent $Mn_{3-\delta}Ga$ layer, grown using $R_F = 0.55$, along different azimuths are shown in Figs. 1(c)–1(f). At the initial stage of $Mn_{3-\delta}Ga$ growth along the GaN[$11\bar{2}0$] azimuth, as seen in Fig. 1(c), we note that $6\times$ diffraction lines appear. After only 5–10 s of growth, the RHEED pattern evolves to that of the $Mn_{3-\delta}Ga(111)$ surface, as seen in Fig. 1(d) in the direction of [$1\bar{1}00$] of GaN, which has already become the [$1\bar{1}0$] direction of $Mn_{3-\delta}Ga$. After a full 1 monolayer of $Mn_{3-\delta}Ga$ growth, the RHEED patterns evolve to the $2\times$ patterns shown in Figs. 1(e) and 1(f), taken after the film had reached a final thickness of ~1100 Å. For $Mn_{3-\delta}Ga$ growth with a smaller flux ratio ($R_F = 0.5$), the growth evolution is the same except that there are no $2\times$ streaks, as shown in Figs. 1(g) and 1(h).

The stoichiometry obtained at $R_F = 0.55$ was found to have Mn:Ga ~ 1.22–1.5:1, corresponding to δ in the range 1.5–1.78 or, equivalently, Mn/(Mn + Ga) composition in the range 0.55–0.6. Such values are very consistent with previous measurements for CuAu-$L1_0$-type fct $Mn_{3-\delta}Ga$ samples prepared using bulk synthesis [13].

In our experiments, the $Mn_{3-\delta}Ga$ RHEED patterns are always streaky for R_F within the range 0.5–0.6 and from the very beginning of MnGa growth, indicating high quality epitaxy of the $Mn_{3-\delta}Ga$ layer on the GaN substrate. Comparing Figs. 1(e) and 1(f) with Figs. 1(a) and 1(b), the in-plane symmetries of the $Mn_{3-\delta}Ga$ layer are clearly reversed from those of the GaN(0001) substrate, corresponding to a 30° rotation of the hexagonal lattice. We thus derive an epitaxial relationship of the $Mn_{3-\delta}Ga$ layer with the GaN(0001) substrate. Shown in Fig. 2(a) is a model of the Ga-terminated, *w*-GaN(0001) surface lattice. Similarly, shown in Fig. 2(b) is a three-dimensional model of the $Mn_{3-\delta}Ga$ fct lattice [13]. From this 3D model, one can derive the top view model of the $Mn_{3-\delta}Ga(111)$ surface, as shown in Fig. 2(c). It consists of an alternating Mn and Ga row structure.

By overlaying the $Mn_{3-\delta}Ga(111)$ lattice onto the GaN(0001) lattice, as shown in Fig. 2(d), we find a nearly perfect epitaxial relationship, with a 30° rotation between the two lattices. This interface model involves the smallest number of high symmetry bonding sites, including Ga bridge, Mn bridge, and Mn atop sites, resulting in an ideal epitaxial fit. Interchange of Ga and Mn overlayer atoms would result in a similar model without affecting the RHEED symmetry.

From the RHEED results, the in-plane lattice parameters of the $Mn_{3-\delta}Ga$ layers are computed to be $a_1 = 2.67$ Å and $a_2 = 2.76$ Å, in good agreement with values deduced

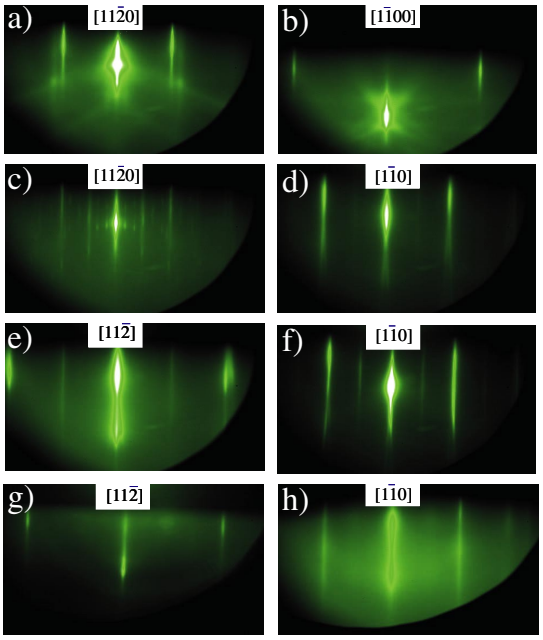

FIG. 1 (color online). RHEED patterns taken from the GaN(0001) substrate and the $Mn_{3-\delta}Ga$ layer during and after the growth. (a),(b) After refreshing the GaN surface with 50 nm GaN by MBE; (c),(d) the initial stage of MnGa growth with $R_F = 0.55$; (e),(f) the later stage of $Mn_{3-\delta}Ga$ growth with $R_F = 0.55$ showing 2×2 reconstruction; (g),(h) same as for (e),(f) but for $R_F = 0.5$. (a)–(d) were acquired at 250 °C; (e)–(h) were acquired at 25 °C.

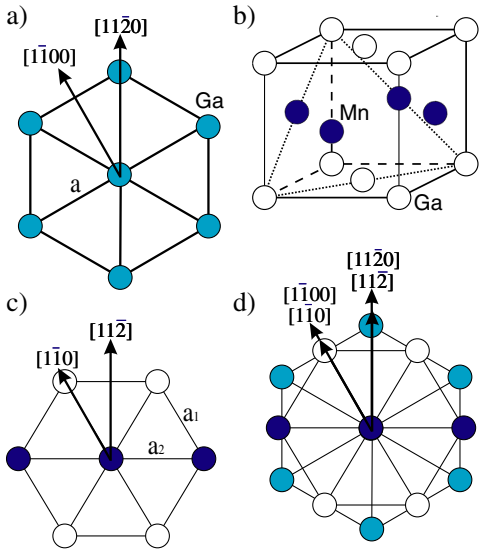

FIG. 2 (color online). (a) Top view of Ga-polar *w*-GaN(0001) showing the top layer as Ga atoms; (b) perspective view of the $Mn_{3-\delta}Ga$ CuAu type-I ($L1_0$) structural model; (c) top view of the $Mn_{3-\delta}Ga(111)$ surface; (d) overlaid models showing the epitaxial relationship of $Mn_{3-\delta}Ga(111)$ to Ga-polar *w*-GaN(0001).

from the known fct lattice parameters [13], which are a_1 = Mn-Ga distance = 2.67 Å and a_2 = Mn-Mn or Ga-Ga distance = 2.756 Å. Negligible difference was found among samples grown with different R_F.

Thus, we have an epitaxial $Mn_{3-\delta}Ga$ layer having the [111] axis perpendicular to the (0001) GaN surface and with the epitaxial relationship $Mn_{3-\delta}Ga(111)[1\bar{1}0] \parallel GaN(0001)[1\bar{1}00]$ and $Mn_{3-\delta}Ga(111)[11\bar{2}] \parallel GaN(0001)[11\bar{2}0]$. The growth orientation of the $Mn_{3-\delta}Ga$ film was confirmed by XRD and RBS ion channeling.

To achieve the high quality $Mn_{3-\delta}Ga(111)$ epitaxial growth on w-GaN(0001) presented here, it is crucial to hold T_{sub} at 250 °C for growth with R_F varying in the range of 0.5–0.6. In this range, the sharp and streaky 6× RHEED pattern always appears at the initial stage of the growth. Such a streaky, reconstructed RHEED pattern suggests a smooth and abrupt $Mn_{3-\delta}Ga/GaN$ interface, which is a key advantage since one of the most desirable properties for any FM/SC system is a smooth and abrupt interface. In most conventional FM/III–V SC systems, interface roughness and interdiffusion are serious problems which typically lead to the formation of interface compounds, even antiferromagnetic (AFM) interface layers. The $Mn_{3-\delta}Ga/GaN$ interface avoids both of these problems. This is due to (a) the strong and stable Ga-N bond which prevents reaction between the anion (N) and the FM overlayer; (b) the chemical compatibility of $Mn_{3-\delta}Ga$ with the well-known gallium-rich surface of MBE-grown w-GaN(0001) [20] which further prevents reactions with N; (c) the high immiscibility of Mn and GaN which further prevents Mn from entering into the GaN layer; and (d) the ideal $Mn_{3-\delta}Ga/GaN(0001)$ epitaxial relationship which prevents interface roughness and promotes two-dimensional epitaxy.

An STM image of the smooth $Mn_{3-\delta}Ga(111)$ surface grown with R_F = 0.55–0.6, of size 300 Å × 300 Å and including several atomic-height terraces, is shown in Fig. 3(a). The height of an individual step is measured to be h = 2.23 Å, in good agreement with the d spacing between $Mn_{3-\delta}Ga(111)$ planes obtained from XRD (~2.20 Å). It is also consistent with the CuAu-$L1_0$-type fct $Mn_{3-\delta}Ga(111)$ interplanar spacing. Zooming in to a smaller area, as shown in Fig. 3(b), the real-space atomic image corresponding to the $\frac{1}{2}$-order RHEED streaks is observed. Although the corrugation is not large, we find a hexagonlike lattice with spacing 2 × 2.7 Å = 5.4 Å.

Thus, we find that the stoichiometry can be determined from the surface reconstruction: 1 × 1 ⇒ 1:1 Mn to Ga, and 2 × 2 ⇒ 3 − δ:1 Mn to Ga, with δ in the range 0–2. The 2 × 2 is therefore an indicator of higher Mn incorporation and other important layer properties.

To understand the origin of the 2 × 2 structure, we reconsider the 1 × 1 occurring for lower flux ratio R_F = 0.5; at the surface, we find alternating rows of Mn and Ga atoms, as shown in Fig. 3(c). The 2 × 2, occurring for $R_F > 0.5$, is then obtained by replacing every other Ga atom with a Mn atom, as shown in Fig. 3(d). If this Mn_{Ga} replacement is continued into the bulk, a Mn:Ga = 3:1 stoichiometry *would* result, equivalent to the Mn_3Ga (δ = 0) phase ⇒75% Mn content. For $0.5 < R_F < 0.75$, we expect only partial replacement, consistent with our RHEED results for Mn:Ga = 1.22–1.5:1 (R_F = 55%–60%), in which we observe weak $\frac{1}{2}$-order streaks.

The magnetic properties of the epitaxial $Mn_{3-\delta}Ga$ films on both Ga-polar and N-polar GaN substrates were investigated by VSM at 25 °C. All films exhibited magnetic anisotropy, based on comparison of VSM hysteresis loops along the perpendicular [111] and parallel $[11\bar{2}]$ and/or $[1\bar{1}0]$ directions. The saturation magnetization M_s, remnant magnetization M_r, and coercivity H_c vary for different samples depending on their compositions. In particular, M_s was found to vary from 250 to 510 emu/cm^3. Previous theoretical and experimental work has confirmed that Mn_xGa_{1-x} is ferromagnetic for Mn content in the range 50%–74.7% [1–3,5,21,22]. Van Roy *et al.* [2] reported M_s decreasing from 510 to 450 emu/cm^3 and T_C increasing with increasing Mn content in the range 56%–59%. Tanaka *et al.* [3] reported two samples, one having M_s = 414 emu/cm^3 with T_C = 327 °C at 56% Mn and another having M_s = 390 emu/cm^3 with Tc = 373 °C at 59% Mn. Also, an M_s = 460 emu/cm^3 at 62% Mn was reported by Krishnan [5].

By tuning the reconstruction during MBE growth, we can control the magnetic properties of the $Mn_{3-\delta}Ga$ layers grown on w-GaN wide band-gap semiconductor and sapphire substrates. Figure 4 shows magnetization vs applied magnetic field for magnetic fields applied both perpendicu-

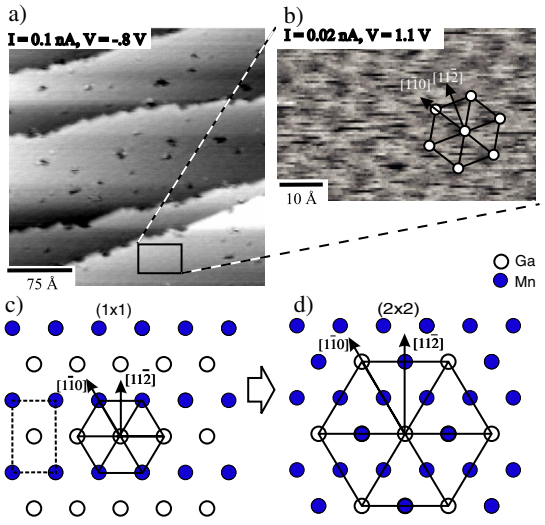

FIG. 3 (color online). (a) 300 Å × 300 Å STM image of 2 × 2-reconstructed $Mn_{3-\delta}Ga(111)$ on w-GaN(0001); (b) 50 Å× 35 Å zoom-in STM image of terrace region shown in (a); (c) surface model of unreconstructed $Mn_{3-\delta}Ga(111)$ having a 1 × 1 unit cell; (d) 2 × 2-reconstructed $Mn_{3-\delta}Ga(111)$ model. Dark spots on terraces in (a) are defects, possibly vacancy islands.

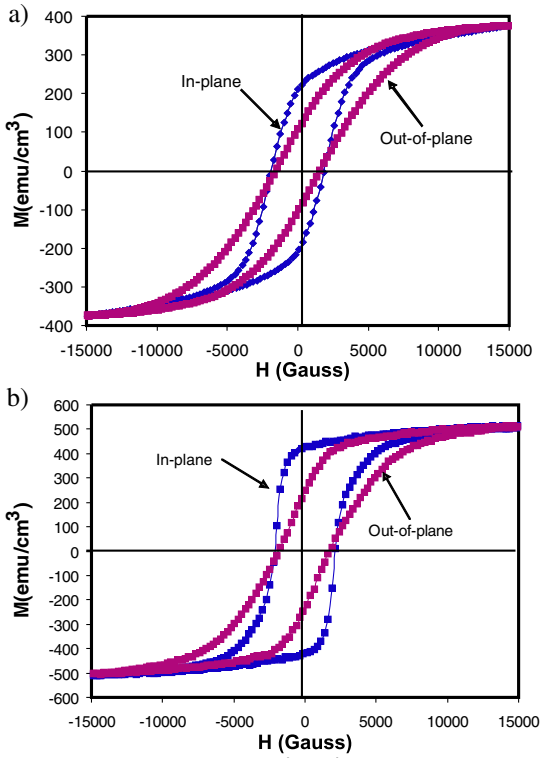

FIG. 4 (color online). VSM magnetization vs applied magnetic field (hysteresis loops) with the field applied parallel and perpendicular to the $Mn_{3-\delta}Ga(111)$ layer, for (a) 1×1-reconstructed $Mn_{3-\delta}Ga(111)$ growth and (b) 2×2-reconstructed $Mn_{3-\delta}Ga(111)$ growth. Measurements were made at room temperature (27 °C).

lar and parallel to the $Mn_{3-\delta}Ga(111)$ thin film surfaces. The hysteresis loops clearly show magnetic anisotropy of the $Mn_{3-\delta}Ga$ thin films for both the 1×1 and 2×2 reconstructions. For the 1×1-reconstructed $Mn_{3-\delta}Ga(111)$ with 50% Mn concentration as seen in Fig. 4(a), $M_s = 375$ emu/cm^3; in this case, $M_r = 207$ emu/cm^3 and $H_c = 1.913$ kOe for the in-plane loop, whereas $M_r = 104$ emu/cm^3 and $H_c = 1.528$ kOe for the out-of-plane loop. For the 2×2-reconstructed $Mn_{3-\delta}Ga(111)$ at 55% Mn concentration as seen in Fig. 4(b), $M_s = 510$ emu/cm^3; in this case, $M_r = 423$ emu/cm^3 and $H_c = 2.168$ kOe for the in-plane loop, whereas $M_r = 247$ emu/cm^3 and $H_c = 1.928$ kOe for the out-of-plane loop. All of our samples show similar anisotropy of M_r and H_c, confirming the epitaxial, crystalline quality of our $Mn_{3-\delta}Ga$ thin films on w-GaN substrates.

The deduced magnetic moments in our $Mn_{3-\delta}Ga$ thin films vary from $m = 0.76\mu_B$/Mn atom at 50% Mn content to $m = 1.88\mu_B$/Mn atom at 55% Mn content. For 60%, we measured only $0.85\mu_B$/Mn atom. Although our experimental moments are among the highest reported, our highest measured value is still lower than the theoretical values of $2.33\mu_B$ and $2.42\mu_B$ per Mn atom for δ-MnGa (Mn:Ga = 1:1) predicted by Yang *et al.* [22] and by Sakuma [21], respectively. As it is reported experimentally that for Mn/(Mn + Ga) fraction $\geq 75\%$, the magnetic moment is very small due to AFM interactions [2], our measured reduction of m over the range from 55% to 60% Mn content may be due to the onset of AFM interactions.

In conclusion, high quality epitaxial growth of ferromagnetic layers of $Mn_{3-\delta}Ga$ with ideal lattice matching having a (111) orientation to w-GaN(0001) or $(000\bar{1})$ and an abrupt interface is reported. The magnetic properties are tuned by adjusting the reconstruction during growth which affects the composition, and the composition change with Mn flux is shown to be detected by the 2×2 reconstruction. Mn atoms fill into Ga sites in an ordered 2×2 arrangement, resulting in Mn:Ga > 1:1 and up to 3:1 at complete Mn filling. The results suggest a gradual transition from the fct (111)-oriented structure to a hexagonal structure. The $Mn_{3-\delta}Ga$/GaN structures are promising for spintronic applications in integrated magnetic-semiconductor devices.

E. L. gratefully acknowledges M. B. Haider and R. Yang for their helpful technical support in the MBE/STM Lab151. This material is based upon work supported by the National Science Foundation under Grants No. 0304314 and No. 9983816. Equipment support from the Office of Naval Research is also acknowledged.

[1] W. Van Roy *et al.*, Appl. Phys. Lett. **69**, 711 (1996).
[2] W. Van Roy, H. Akinaga, and S. Miyanishi, Phys. Rev. B **63**, 184417 (2001).
[3] M. Tanaka *et al.*, Appl. Phys. Lett. **62**, 1565 (1993).
[4] M. Tanaka *et al.*, Appl. Phys. Lett. **63**, 696 (1993).
[5] K. M. Krishnan, Appl. Phys. Lett. **61**, 2365 (1992).
[6] J. L. Hilton *et al.*, Appl. Phys. Lett. **84**, 3145 (2004).
[7] M. B. Haider *et al.*, J. Appl. Phys. **93**, 5274 (2003).
[8] S. J. Pearton *et al.*, J. Phys. Condens. Matter **16**, R209 (2004).
[9] K. H. Kim *et al.*, Appl. Phys. Lett. **82**, 1775 (2003).
[10] J. P. Zhang *et al.*, Appl. Phys. Lett. **71**, 143 (1997).
[11] M.-H. Ham, S. Yoon, Y. Park, L. Bian, M. Ramsteiner, and J.-M. Myoung, J. Phys. Condens. Matter **18**, 7703 (2006).
[12] S. A. Wolf, D. D. Awschalom, R. A. Buhrman, J. M. Daughton, S. von Molnar, M. L. Roukes, A. Y. Chtchelkanova, and D. M. Treger, Science **294**, 1488 (2001).
[13] H. Niida *et al.*, J. Appl. Phys. **79**, 5946 (1996).
[14] J. S. Wu and K. H. Kuo, Metall. Mater. Trans. A **28**, 729 (1997).
[15] O. Gourdon and G. J. Miller, J. Solid State Chem. **173**, 137 (2003).
[16] T. Matsui *et al.*, J. Appl. Phys. **73**, 6683 (1993).
[17] V. Prudnikov *et al.*, J. Magn. Magn. Mater. **188**, 393 (1998).
[18] M. Ishii, S. Iwai, T. Ueki, and Y. Aoyagi, J. Cryst. Growth **187**, 234 (1998).
[19] S. J. Pearton *et al.*, J. Electron. Mater. **32**, 288 (2003).
[20] A. R. Smith, R. M. Feenstra, D. W. Greve, M.-S. Shih, M. Skowronski, J. Neugebauer, and J. E. Northrup, J. Vac. Sci. Technol. B **16**, 2242 (1998).
[21] A. Sakuma, J. Magn. Magn. Mater. **187**, 105 (1998).
[22] Z. X. Yang *et al.*, J. Magn. Magn. Mater. **182**, 369 (1998).